

Discovery and Characterization of Vicriviroc (SCH 417690), a CCR5 Antagonist with Potent Activity against Human Immunodeficiency Virus Type 1

Julie M. Strizki, Cecile Tremblay, Serena Xu, Lisa Wojcik, Nicole Wagner, Waldemar Gonsiorek, R. William Hipkin, Chuan-Chu Chou, Catherine Pugliese-Sivo, Yushi Xiao, Jayaram R. Tagat, Kathleen Cox, Tony Priestley, Steve Sorota, Wei Huang, Martin Hirsch, Gregory R. Reyes and Bahige M. Baroudy
Antimicrob. Agents Chemother. 2005, 49(12):4911. DOI: 10.1128/AAC.49.12.4911-4919.2005.

Updated information and services can be found at:
<http://aac.asm.org/content/49/12/4911>

REFERENCES

These include:

This article cites 25 articles, 12 of which can be accessed free at: <http://aac.asm.org/content/49/12/4911#ref-list-1>

CONTENT ALERTS

Receive: RSS Feeds, eTOCs, free email alerts (when new articles cite this article), [more»](#)

Information about commercial reprint orders: <http://journals.asm.org/site/misc/reprints.xhtml>
To subscribe to to another ASM Journal go to: <http://journals.asm.org/site/subscriptions/>

Discovery and Characterization of Vicriviroc (SCH 417690), a CCR5 Antagonist with Potent Activity against Human Immunodeficiency Virus Type 1

Julie M. Strizki,^{1*} Cecile Tremblay,² Serena Xu,¹ Lisa Wojcik,¹ Nicole Wagner,¹ Waldemar Gonsiorek,³
R. William Hipkin,³ Chuan-Chu Chou,³ Catherine Pugliese-Sivo,³ Yushi Xiao,⁴ Jayaram R. Tagat,⁴
Kathleen Cox,⁵ Tony Priestley,⁶ Steve Sorota,⁶ Wei Huang,⁷ Martin Hirsch,²
Gregory R. Reyes,¹ and Bahige M. Baroudy¹

*Departments of Antiviral Therapy,¹ Inflammation,³ Medicinal Chemistry,⁴ Drug Metabolism and Pharmacokinetics,⁵
and Neurobiology,⁶ Schering-Plough Research Institute, Kenilworth, New Jersey 07033; Infectious Disease Division,
Department of Medicine, Massachusetts General Hospital, Fruit Street, Boston, Massachusetts 02114²; and
Monogram Biosciences, 345 Oyster Point Boulevard, South San Francisco, California 94080⁷*

Received 14 April 2005/Returned for modification 7 July 2005/Accepted 27 September 2005

Inhibiting human immunodeficiency virus type 1 (HIV-1) infection by blocking the host cell coreceptors CCR5 and CXCR4 is an emerging strategy for antiretroviral therapy. Currently, several novel coreceptor inhibitors are being developed in the clinic, and early results have proven promising. In this report, we describe a novel CCR5 antagonist, vicriviroc (formerly SCH-D or SCH 417690), with improved antiviral activity and pharmacokinetic properties compared to those of SCH-C, a previously described CCR5 antagonist. Like SCH-C, vicriviroc binds specifically to the CCR5 receptor and prevents infection of target cells by CCR5-tropic HIV-1 isolates. In antiviral assays, vicriviroc showed potent, broad-spectrum activity against genetically diverse and drug-resistant HIV-1 isolates and was consistently more active than SCH-C in inhibiting viral replication. This compound demonstrated synergistic anti-HIV activity in combination with drugs from all other classes of approved antiretrovirals. Competition binding assays revealed that vicriviroc binds with higher affinity to CCR5 than SCH-C. Functional assays, including inhibition of calcium flux, guanosine 5'-[³⁵S]triphosphate exchange, and chemotaxis, confirmed that vicriviroc acts as a receptor antagonist by inhibiting signaling of CCR5 by chemokines. Finally, vicriviroc demonstrated diminished affinity for the human ether a-go-go related gene transcript ion channel compared to SCH-C, suggesting a reduced potential for cardiac effects. Vicriviroc represents a promising new candidate for the treatment of HIV-1 infection.

The first stage in the human immunodeficiency virus type 1 (HIV-1) life cycle is comprised of a series of sequential events that occur at the cell surface prior to viral entry and infection. These steps include binding of the viral envelope gene, gp120, to the cellular CD4 receptor, engagement of the cellular coreceptor (CCR5 or CXCR4), and membrane fusion mediated by the viral gp41 protein (4, 5). Blocking these early events in HIV infection has proven to be an attractive target for antiviral intervention, and numerous entry inhibitors are currently being developed as novel therapies (5, 7). Among the first entry inhibitors to be identified were peptide-based inhibitors of gp41 that acted by blocking membrane fusion, thus preventing viral infection (20, 26). Two fusion inhibitors, enfuvirtide and T-1249, have shown potent antiviral activity in the laboratory and proven efficacy in the clinic (6, 12, 14). More recently, agents that target the gp120-CD4 interaction (11, 15) or subsequent engagement of cellular coreceptors have been described and are being developed as antiretrovirals (4, 7, 16). In particular, antagonists of the cellular coreceptors, CCR5 and CXCR4, have shown promise in early-phase clinical trials (10, 13, 16).

One of the first small-molecule CCR5 antagonists to be described was SCH-C (SCH 351125) (17, 21). This compound was shown to selectively bind to CCR5 and effectively inhibit replication of a broad range of HIV-1 isolates that utilize this coreceptor for infection (termed R5 tropic) (21). In a proof-of-concept clinical trial, SCH-C reduced plasma viral RNA titers in HIV-1-infected patients by 1.5 logs when dosed orally at 100 mg twice daily for 10 days, thus validating CCR5 as a target for intervention against HIV-1 infection (D. Schurmann, R. Rouzier, R. Nougarede, J. Reynes, G. Fatkenheuer, R. Raffi, C. Michelet, A. Tarral, C. Hoffmann, J. Kiunke, H. Sprenger, J. van Lier, A. Sansone, M. Jackson, and M. Laughlin, Abstr. 11th Conf. Retrovir. Opportun. Infect., abstr. 140LB, 2004).

Although SCH-C demonstrated potent antiviral activity and excellent oral bioavailability and was well tolerated in the clinic, this compound caused a modest but dose-dependent prolongation of the corrected cardiac QT interval (QTc) in test subjects. This effect may be related to the moderate binding affinity of SCH-C for the human ether a-go-go related gene transcript (hERG), a potassium ion channel associated with myocardial repolarization (8, 19). Therefore, in order to identify a backup candidate to follow SCH-C, we selected compounds exhibiting superior antiviral and pharmacokinetic properties compared to those earlier generation compounds as well as a reduced tendency for hERG channel blockade. In the current report we describe the characterization of a second

* Corresponding author. Mailing address: Schering-Plough Research Institute, Antiviral Therapy, 2015 Galloping Hill Road, K15, E405C/4945, Kenilworth, NJ 07033. Phone: (908) 740-4731. Fax: (908) 740-3032. E-mail: Julie.strizki@spcorp.com.

CCR5 antagonist, vicriviroc (previously known as SCH-D or SCH 417690), that has a superior overall profile compared to that of the prototypic CCR5 antagonist, SCH-C.

MATERIALS AND METHODS

Compounds. The chemical syntheses of SCH-C (SCH 351125) and vicriviroc (SCH-D, or SCH 417690) have been previously described (17, 22, 23). Other antiviral compounds, zidovudine and lamivudine (Glaxo SmithKline, Inc., Research Triangle Park, NC), efavirenz (Bristol-Myers Squibb Co., Wallingford, CT), indinavir (Merck & Co, Inc., West Point, PA), and enfuvirtide (Trimeris, Durham, NC), were provided to Harvard Medical School by their respective manufacturers. RANTES, MIP-1 α , and MIP-1 β were obtained from R&D Systems (Minneapolis, MN).

Virus stocks and reagents. Primary clade B and nonclade B HIV-1 isolates were obtained from the National Institutes of Health (NIH) AIDS Research and Reference Reagent Program, Division of AIDS, and the World Health Organization. Other HIV-1 isolates were obtained from Cheryl Stoddart [Ba-L (G); Gladstone Institute, San Francisco, CA], John Moore (ADA-M and JR-FL; Cornell Medical College, New York, NY), and Martin Markowitz (HJE155, nelfinavir resistant; Aaron Diamond AIDS Research Center, New York, NY). The CCR5-tropic clinical HIV-1 isolate R5-01 used for the drug combination studies was derived from a subject with acute HIV-1 primary infection syndrome at the Massachusetts General Hospital.

PBMC replication assay. Ficoll-purified peripheral blood mononuclear cells (PBMCs) were stimulated in vitro with phytohemagglutinin (PHA) (Sigma, St. Louis, MO) (5 μ g/ml) and interleukin-2 (IL-2) (50 U/ml) (NIH AIDS Research and Reference Reagent Program) for 3 to 7 days. The cells were resuspended at 4×10^6 /ml in complete medium (RPMI, 10% fetal bovine serum [FBS], 50 U/ml IL-2), seeded into 96-well plates (2×10^5 /well), incubated with an equal volume of culture medium containing compound for 1 h at 37°C, and infected in triplicate with 25 to 100 50% tissue culture infectious doses (TCID₅₀) per well of viral inoculum for 3 to 4 h. Cells were washed twice in phosphate-buffered saline (PBS) to remove residual virus and were cultured with compound for 4 to 6 days. HIV-1 replication was quantified by measurement of extracellular p24 antigen in the supernatants by enzyme-linked immunosorbent assay (Perkin Elmer). The 50% effective concentrations (EC₅₀s) and EC₉₀s for each virus were determined using GraphPad PRISM software (Intuitive Software for Science, San Diego, CA).

PhenoSense HIV-1 entry assay. A rapid infectivity assay (18) was used to measure the drug susceptibility of recombinant pseudoviruses that carry drug resistance mutations in the reverse transcriptase (RT), protease (PR), and/or gp41 genes. Pseudotyped recombinant viruses were generated by cotransfecting HEK293 cells with an HIV-1 genomic vector containing a luciferase reporter cassette and envelope expression vectors containing the gp160 sequence from HIV JrCSF or a mutated JrCSF envelope engineered to contain the V38A or G36D and V38M enfuvirtide resistance mutations in gp41 (9). Alternatively, pseudoviruses resistant to RT and/or PR inhibitors were generated by transfection of HIV-1 genomic plasmids containing multiple RT or PR drug resistance mutations with a wild-type JrCSF envelope plasmid. Virus stocks were harvested 48 h after transfection and used to inoculate U87-CD4-CCR5 target cells, either in the absence or presence of serial dilutions of vicriviroc. Infection was determined by measuring luciferase activity in target cells 72 h after inoculation and inhibition, calculated with the following equation: $[1 - (\text{luciferase activity in the presence of the drug/luciferase activity in the absence of the drug})] \times 100$. The data were analyzed by plotting the percent inhibition of luciferase activity (y axis) versus the log₁₀ drug concentration (x axis).

Drug combination studies. PBMC from HIV-1-seronegative donors were stimulated with PHA for 3 days and resuspended at a concentration of 1×10^6 cells/ml in RPMI 1640 culture medium (Sigma) supplemented with 20% heat-inactivated FBS (Sigma), penicillin (50 U/ml), streptomycin (50 μ g/ml), L-glutamine (2 mM), HEPES buffer (10 mM), and human IL-2 (100 U/ml) in 24-well tissue culture plates (Becton Dickinson, San Jose, Calif.). Single drugs or combinations of drugs were added to each well, using a fixed ratio between drugs and serial dilutions, simultaneously with the HIV-1 inoculum (1,000 to 5,000 50% TCID₅₀/10⁶ cells), and plates were incubated at 37°C. Each condition was tested in duplicate, and each experiment was repeated at least twice. Cell-free culture supernatants were harvested and analyzed by enzyme-linked immunosorbent assay (Perkin Elmer) for HIV-1 p24 antigen production on day 7 of culture. In addition, uninfected drug-treated cytotoxicity controls were maintained at the highest concentration of each agent tested. Cell proliferation and viability were assessed by the trypan blue dye exclusion method.

Mathematical analysis. The multiple-drug effect analysis of Chou, based on the median effect principle and the isobologram technique, was used to analyze combined-drug effects (2). This method plots dose-effect curves for each drug and for multiply diluted fixed-ratio combinations of drug by using the median-effect equation. The slope of the median-effect plot, which signifies the shape of the dose-effect curve, and the x intercept of the plot, which signifies the potency of each compound and each combination, are used for a computerized calculation of a combination index. A mutually exclusive model of analysis was used. Combination indices of <0.9 indicate synergy (i.e., greater than the expected additive effect when two agents are combined), combination indices of 0.9 to 1.1 indicate nearly additive effects, and a combination index of >1.1 indicates antagonism (i.e., less than the expected additive effect).

Membrane binding. Radioligand competition and saturation binding assays were done using scintillation proximity assay (SPA) technology. Membranes (1 to 2 μ g per assay point) from HTS1 cells expressing human CCR5 (Stratagene, La Jolla, CA) in SPA binding buffer (50 mM TRIS, 100 mM NaCl, 10 mM MgCl₂, 1 mM EDTA, 0.1% bovine serum albumin [BSA], pH 7.6) were preincubated for 30 min at room temperature with 200 μ g wheat germ agglutinin-coated SPA beads (WGA-SPA; Amersham, Arlington Heights, IL), transferred to a 96-well isoplate, and further incubated at room temperature with the indicated concentrations of [³H]SCH-C and specified dilutions of SCH-C and/or vicriviroc. Competition and saturation binding analyses were analyzed using GraphPad PRISM software (Intuitive Software for Science). Ligand affinities from competition experiments were calculated from binding 50% inhibitory concentrations (IC₅₀s) using the Cheng-Prusoff equation (1).

Calcium flux assay. U-87-CCR5 cells were plated 2 days prior to testing at a concentration of 15,000 cells/well in culture medium (Dulbecco's modified Eagle medium supplemented with 10% FBS). On the day of the assay, the culture medium was removed and replaced with 100 μ l of flux buffer (0.71 mg/ml Probenecid, 20 mM HEPES, 0.1% BSA in Hanks balanced salt solution) containing 5 mg/ml of the calcium-sensitive dye, Fluo4 (Molecular Probes, Eugene, OR). The plates were incubated for 1 h at 37°C and then washed once with flux buffer. Compounds were serially diluted in flux buffer and added to quadruplicate wells; calcium signaling was measured immediately using a Fluorometric Imaging Plate Reader (FLIPR; Molecular Devices, Sunnyvale, CA). Following the initial FLIPR read, the chemokines RANTES, MIP-1 α , and MIP-1 β were added to the cells (10 nM final concentration) and calcium levels were again determined. The advantage of this two-read procedure is that it provides an indication of any intrinsic activity associated with the test compound (first read) in addition to estimating antagonist (IC₅₀) activity following addition of a chemokine agonist (second read). Calcium signals in individual wells were calculated as the maximum fluorescence reading following addition of ligand minus the minimum fluorescence reading before addition of ligand. The percent of calcium flux was calculated by the following equation: $[(\text{calcium signal in compound treated wells})/(\text{calcium signal in RANTES only treated wells})] \times 100$. The IC₅₀s for SCH-C and vicriviroc were calculated using standard curve-fitting routines (GraphPad Prism software).

Chemotaxis assay. Ba/F3-CCR5 cells (2.5×10^6 cells/ml) in chemotaxis buffer (RPMI supplemented with 1% FBS and 0.1 μ g/ml mouse IL-3) were pretreated for 1 h with decreasing concentrations of vicriviroc or SCH-C at 37°C. Chemotaxis buffer containing compound and MIP-1 α (0.3 nM), MIP-1 β (0.3 nM), or RANTES (0.3 nM) was placed into the bottom well of a 5- μ m ChemoTx plate (Neuroprobe, Inc.), and the filter unit was placed over the wells. Ba/F3-CCR5 cells pretreated with compounds were pipetted (25 μ l) onto the filters, and the plate was incubated at 37°C for 2 h. Unmigrated cells were scraped off the filter, and the plate was centrifuged to pellet-migrated cells. Cells were then transferred to a Microtiter 1+ Flatbottom Microtiter (Thermo Labsystems, Franklin, MA) plate and quantitated using the Cell Titer Glow luminescent cell viability assay kit (Promega, Madison, WI). IC₅₀s for each compound were calculated using GraphPad Prism Software (Intuitive Software for Science).

[³⁵S]GTP γ S binding assay. Exchange of guanosine 5'-[³⁵S]triphosphate ([³⁵S]GTP γ S, triethylammonium salt; specific activity, 1,250 Ci/mmol; NEN, Boston, MA) was measured using a scintillation proximity assay (SPA) as previously described by Cox et al. (3). For each assay point, 2 μ g of HTS1-hCCR5 membrane was preincubated for 30 min at room temperature with 200 μ g of WGA-SPA beads in SPA binding buffer (50 mM HEPES, 10 mM MgCl₂, 1 mM EDTA, 100 mM NaCl, 0.1% BSA, pH 7.6). The beads and membranes were transferred to a 96-well isoplate (Wallac, Gaithersburg, MD) and incubated with compounds for 24 h at 4°C. The incubation was then continued at room temperature for 60 min with 10 μ M GDP and 1 nM RANTES. Following the addition of 0.1 nM [³⁵S]GTP γ S for another 60 min, membrane-bound [³⁵S]GTP γ S was measured using a 1450 Microbeta Trilux counter (Wallac, Gaithersburg, MD).

Pharmacokinetic analysis. The *in vivo* pharmacokinetic analysis of SCH-C was previously described (21). Similar techniques were used to evaluate the pharmacokinetic properties of vicriviroc in this study. Briefly, male rats (groups of three) were dosed with [^3H]vicriviroc at 10 mg/kg of body weight by either intravenous (i.v.) injection or oral gavage. In the monkey studies, three fasted male cynomolgus monkeys were dosed intravenously or orally at 2 mg per kg (mpk). The compound was dissolved in 0.4% methylcellulose for oral dosing and in 20% hydroxypropyl- β -cyclodextrin for i.v. dosing. Following compound administration, plasma samples were collected periodically over 24 h. Plasma samples were subjected to protein precipitation, and the supernatant was injected into a high-performance liquid chromatography tandem mass spectrometric detection system. Parent compound was quantified against a standard curve, area under the curve (AUC) was calculated from the concentration versus time profiles, and the pharmacokinetic parameters were calculated by using the Watson LIMS system. Total radioactivity in the plasma samples was measured by scintillation counting, and a concentration-equivalent-versus-time profile was determined. Absorption was calculated from the relative AUC ratios of the i.v. and oral gavage total radioactivity concentration-equivalents-versus-time profiles.

Compound binding to human plasma proteins was evaluated by spiking the compound into the plasma samples at 0.94 μM . Separation of free drug from protein-bound material was achieved by filtration of the sample through an ultrafiltration membrane.

The inhibition potential, including metabolism-based inhibition, of vicriviroc in human liver microsomes was evaluated by incubation of compound with human liver microsomes, NADPH, and substrates specific for inhibition of CYP2D6, CYP3A4, CYP2C9, CYP2C19, and CYP1A2. Metabolism-based inhibition of these enzymes was determined following a 30-min preincubation of vicriviroc in human liver microsomes.

hERG assay. Whole-cell voltage clamp experiments were performed to determine the effect of vicriviroc at the hERG potassium channel. Mouse L-929 cells, stably expressing recombinant hERG ion channels, were transferred to a perfused chamber on a Zeiss Axiovert microscope. The composition of the HEPES-buffered superfused salt solution was as follows: 144 mM NaCl, 11 mM glucose, 10 mM HEPES-NaOH, 5.4 mM KCl, 1.8 mM CaCl_2 , 1 mM MgCl_2 . Temperature was maintained at 35°C, and pH was adjusted to 7.4. Individual cells were voltage clamped using an Axopatch-1D amplifier and glass micropipettes filled with the following solution: 140 mM KCl, 10 mM HEPES-NaOH, 5 mM EGTA, 3 mM Mg-ATP, 0.3 mM MgCl_2 (pH 7.2). Initial pipette resistances were between 1.5 to 2.2 M Ω , series resistances were continuously monitored (<10 M Ω), and whole-cell hERG currents were elicited by voltage command pulses to 0 mV from a holding potential of -70 mV at a frequency of 0.1 Hz. Drug effects were evaluated using the deactivating (tail) current upon repolarization to -60 mV as a index of hERG current. Pilot experiments determined that 5-min drug perfusions were sufficient to achieve equilibrium hERG block, control (vehicle-only) experiments revealed gradual rundown in current amplitude, and drug effects were corrected for mean rundown experienced during control experiments.

RESULTS

Through medicinal chemistry as well as pharmacokinetic and biological activity assessments, we identified the small-molecule CCR5 antagonist, vicriviroc (SCH-D or SCH 417690), as a clinical candidate for HIV therapy. The structure of both SCH-C and vicriviroc are shown in Fig. 1. SCH-C is an oxime piperidine compound with a molecular weight of 557. Vicriviroc was selected from a series of piperazine core compounds which also showed good activity in membrane binding and cell-based antiviral assays. The molecular weight of the free base is 533.

Vicriviroc is a CCR5 receptor antagonist. In order to determine if vicriviroc is a receptor agonist or antagonist, three functional assays were employed to measure the ability of the compound to block β -chemokine signaling in CCR5-expressing cells. A chemotaxis assay was first employed to determine the ability of vicriviroc to inhibit chemokine-mediated migration of a mouse Ba/F3 cell line stably expressing recombinant human CCR5. In this assay, vicriviroc and SCH-C showed equally potent inhibition of the chemotactic response to

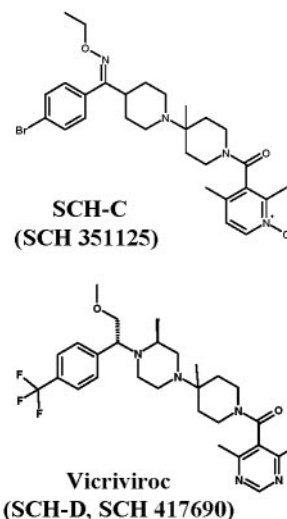


FIG. 1. Structure of SCH-C (SCH 351125) and vicriviroc (SCH-D or SCH 417690).

MIP-1 α with IC_{50} values below 1 nM (Fig. 2A). Similar results were obtained when RANTES and MIP-1 β were used to induce chemotaxis (data not shown).

The ability of vicriviroc to inhibit intracellular calcium release induced by receptor stimulation was also assessed. U-87-CCR5 cells were loaded with the calcium-sensitive dye, Fluo4, prior to addition of vicriviroc or SCH-C, and baseline fluorescence was read. CCR5 signaling was then induced by the addition of RANTES and calcium mobilization was measured as the change in emission spectrum between the calcium-bound and -free forms of the Fluo4 dye. In this assay, both vicriviroc and SCH-C blocked calcium release induced by the ligand RANTES with similar potencies (Fig. 2B). MIP-1 α - and MIP-1 β -induced signaling were also inhibited equally by both compounds (data not shown). Addition of either SCH-C or vicriviroc alone did not stimulate the release of calcium in the U-87-CCR5 cells (data not shown), indicating the lack of intrinsic agonist activity.

A third assay utilized to demonstrate the ability of vicriviroc to inhibit CCR5 receptor signaling was a GTP γS exchange assay. In this assay, cell membranes expressing CCR5 were incubated with compound prior to the addition of [^{35}S]GTP γS and ligand. Receptor activation in response to agonist binding promotes an increased exchange of GDP with radiolabeled GTP at the receptor's cognate G protein α subunit. In the presence of an antagonist, ligand stimulation of GDP-[^{35}S]GTP γS will be inhibited in a concentration-dependent manner. Figure 2C shows the results from a representative experiment comparing the ability of vicriviroc and SCH-C to inhibit GTP γS binding induced by RANTES. Both SCH-C and vicriviroc potently inhibited RANTES-induced signaling with mean IC_{50} s of 10 ± 1.2 nM and 4.2 ± 1.3 nM, respectively. Importantly, neither compound alone induced a signal in this assay (data not shown), thereby confirming the antagonist properties of these compounds.

Taken together, the results of the calcium flux, chemotaxis, and GTP γS assays clearly demonstrate that vicriviroc is a po-

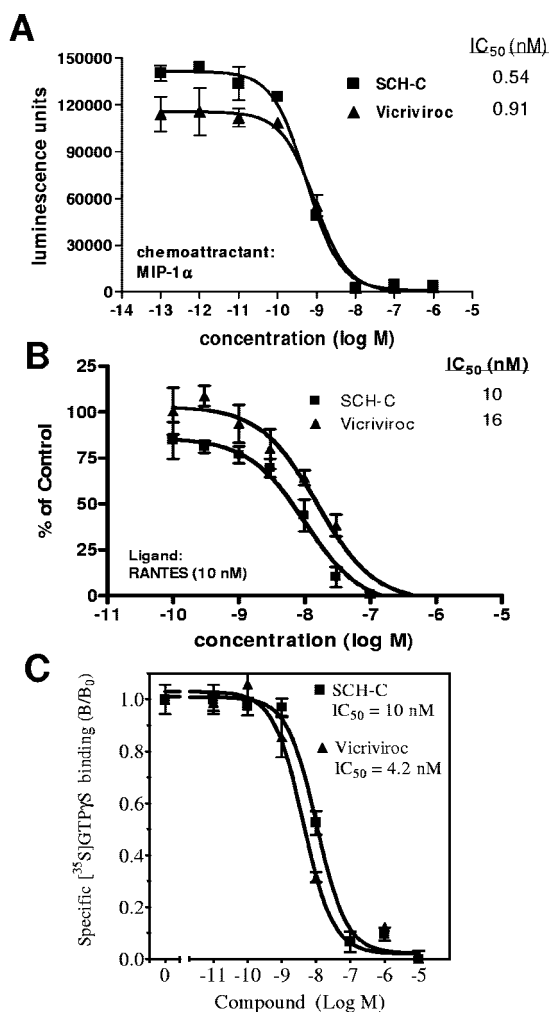


FIG. 2. Inhibition of CCR5 function by vicriviroc. (A) Chemotaxis assay. Ba/F3-CCR5 cells incubated in the presence or absence of antagonists were induced to migrate through a 5- μ m ChemoTx filter by MIP-1 α (0.3 nM). Cell migration was measured by quantifying the number of cells migrating through the membrane using the Cell Titer Glow luminescence kit. The data from a representative experiment are expressed in relative luminescence units, and each point represents an average of 3 wells (\pm standard deviations [SD]). Both SCH-C and vicriviroc inhibited migration of the cells with similar efficacy. (B) Ca flux assay. U-87-CCR5 cells in 96-well plates were loaded with the calcium-sensitive dye Fluo4. Compounds or buffer alone was added to the cells at the indicated concentrations, and calcium signal was immediately read on the FLIPR. The cells were incubated with compound for an additional 5 min prior to the addition of 10 nM RANTES, and the plates were again read on the FLIPR. Data are expressed as the mean (\pm SD) percentage of calcium signal obtained following addition of RANTES in compound-treated wells ($n = 4$) compared with no compound control wells (RANTES only). Both compounds inhibited calcium signaling with similar potency in a dose-dependent fashion. Calcium signal measured in wells treated with SCH-C or vicriviroc alone were similar to background (no RANTES) controls. Data shown are representative of four experiments. (C) GTP γ S binding assay. Membranes (4 μ g/well) from HTS-hCCR5 cells were incubated in binding buffer in the presence of the indicated concentrations of SCH-C or vicriviroc for 24 h at 4°C. The samples were warmed to room temperature and further incubated with 3 μ M GDP and 1 nM RANTES for 1 h. Following the addition of 0.1 nM [35 S]GTP γ S, the incubation continued for 1 h. [35 S]GTP γ S binding to the membranes was measured by WGA-SPA scintillation. Data represent the mean specific binding \pm standard errors of the means of triplicate determinations from a representative experiment ($n = 3$).

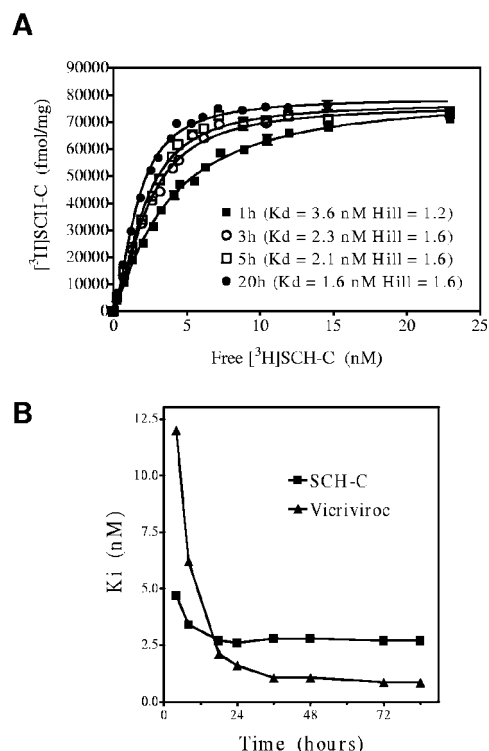


FIG. 3. Saturation and competition binding analysis of hCCR5 with [3 H]SCH-C. (A) Membranes (1 μ g/well) from HTS-hCCR5 cells were incubated for the indicated times in binding buffer with increasing concentrations of [3 H]SCH-C in the absence (total binding) or presence of 1 μ M SCH-C (nonspecific binding). Radioligand binding to the membranes was measured by WGA-SPA scintillation. Data represent the mean specific binding \pm standard errors of the means of triplicate determinations from a representative experiment ($n = 2$). (B) Membranes (2 μ g/well) from HTS-hCCR5 cells were incubated in binding buffer containing 4 nM [3 H]SCH-C and the indicated concentrations of SCH-C and vicriviroc. Radioligand binding to the membranes was measured by WGA-SPA scintillation. The Cheng-Prusoff equation (1) was used to calculate compound affinities from binding IC_{50} at the indicated times. Data from representative experiments ($n = 2$) represent the compound K_i relative to incubation time.

tent antagonist of the CCR5 receptor that is capable of inhibiting receptor function.

Binding studies with [3 H]SCH-C. A [3 H]SCH-C competitive binding assay was used to measure the binding affinity of vicriviroc to CCR5. Saturation analysis (Fig. 3A) showed that [3 H]SCH-C reaches equilibrium binding only after prolonged incubation at room temperature (~ 24 h) and binds with somewhat higher affinity ($K_d = 1.25 \pm 0.55$ nM) than had been described previously ($K_d = 9$ nM) using shorter incubation times in cells (21). In order to define the relative affinities of vicriviroc and SCH-C for CCR5 more precisely, competitive binding analyses were performed using [3 H]SCH-C and binding affinities were calculated at different incubation times. As shown in Fig. 3B, the calculated affinity of vicriviroc is lower than that for SCH-C during early time points, i.e., up to 8 h. However, with more prolonged incubations (~ 24 h) to ensure equilibrium, it is apparent that vicriviroc binds with about threefold higher affinity ($K_i = 0.8$ nM) than does SCH-C ($K_i = 2.6$ nM).

TABLE 1. Vicriviroc inhibits replication of diverse HIV-1 isolates in PBMCs

Virus	Clade/origin	No. of expt	Geometric mean (95% CI) EC (in nM) ^a	
			EC ₅₀	EC ₉₀
93RW023	A/Rwanda	2	0.15 (0.11–0.19)	1.6 (1.1–2.5)
93RW034	A/Rwanda	4	0.13 (0.06–0.24)	1.2 (0.7–2.0)
301657	B/United States	10	1.1 (0.44–3.0)	11 (4.1–30)
302072	B/United States	6	0.37 (0.06–2.5)	3.3 (0.5–22)
ADA-M	B/United States	9	0.40 (0.21–0.78)	4.5 (1.8–12)
ASJM 108	B/United States	7	0.25 (0.14–0.46)	3.3 (1.4–7.5)
ASM 57	B/United States	11	0.55 (0.21–1.5)	4.6 (2.0–11)
ASM 80	B/United States	9	1.1 (0.43–3.2)	8.0 (4.2–15)
ASM 79	B/United States	4	0.46 (0.23–0.93)	8.6 (3.8–19)
Bal (G)	B/United States	20	1.1 (0.61–1.8)	8.0 (4.2–15)
HJE155	B/United States	4	0.18 (0.09–0.4)	1.5 (0.76–3.1)
JRCSF	B/United States	18	1.4 (0.74–2.6)	11 (6.0–19)
JRFL	B/United States	18	0.36 (0.24–0.56)	3.9 (2.2–6.9)
QZ4589	B/Trinidad	15	2.3 (0.89–6.1)	18 (8.5–38)
93IN905	C/India	2	0.21 (0.12–0.39)	1.4 (0.87–2.3)
93IN999	C/India	2	0.11 (0.05–0.28)	1.1 (0.36–3.6)
93MW959	C/Malawi	5	0.29 (0.13–0.62)	3.1 (0.99–9.6)
93MW960	C/Malawi	5	0.34 (0.15–0.75)	3.8 (2.2–6.4)
97ZA003	C/Zaire	3	0.4 (0.06–2.5)	3.5 (0.68–18)
97ZA009	C/Zaire	2	0.5 (0.07–3.8)	4.7 (0.88–25)
98TZ017	C/Tanzania	2	0.12 (0.04–0.34)	1.6 (0.42–5.7)
94UG118	D/Uganda	2	0.09 (0.05–0.18)	1.1 (0.88–1.5)
93UG082	D/Uganda	4	0.17 (0.04–0.72)	1.8 (0.43–7.7)
93TH062	E/Thailand	2	0.25 (0.13–0.48)	2.3 (1.4–3.8)
93TH072	E/Thailand	2	0.25 (0.1–0.62)	2.2 (1.2–4.1)
93TH073	E/Thailand	2	0.04 (0.003–0.55)	0.45 (0.09–2.2)
G3	G/Nigeria	4	0.55 (0.2–1.5)	9.7 (2.1–46)
JV1083	G/Nigeria	17	1.3 (0.78–2.0)	12 (6.8–22)
R132	G/Russia	2	0.55 (0.04–7.9)	4.5 (0.24–84)
RU570	G/Russia	10	1.2 (0.53–2.8)	16 (5.8–42)

^a Values represent the geometric mean EC₅₀ and EC₉₀ values from the indicated number of experiments for each isolate.

Antiviral potency of vicriviroc. The antiviral activity of vicriviroc was evaluated using a PBMC infection assay with a panel of 30 R5-tropic HIV-1 isolates from different regions of the world, representing diverse genetic clades. Each isolate was

tested for susceptibility to vicriviroc in several independent experiments using pooled cells from at least two different uninfected healthy donors. The mean EC₅₀s and EC₉₀s for each isolate are summarized in Table 1. Vicriviroc potentially inhibited all the viral isolates tested, with geometric mean EC₅₀s ranging between 0.04 nM and 2.3 nM and IC₉₀s between 0.45 nM and 18 nM. As expected, viruses capable of using the CXCR4 coreceptor (R5/X4 or X4 tropic) for infection were not significantly inhibited in primary PBMC cultures by vicriviroc (data not shown).

Comparative antiviral activity of vicriviroc and SCH-C. Since differences in the individual donor cells and viral isolates contribute to the variability of the viral replication assay, it can be difficult to assess the relative potency of different compounds tested in independent experiments. Therefore, to directly compare the antiviral activities of vicriviroc with the earlier generation compound, SCH-C, the two compounds were assayed simultaneously using cells from the same donors infected with similar viral inocula. Under these conditions, vicriviroc was consistently more potent (2- to 40-fold) than SCH-C against all of the isolates tested (Fig. 4). Vicriviroc was also highly active against a Clade G Russian isolate, RU570 (Table 1), which previously was shown to be relatively less susceptible to inhibition by SCH-C (EC₉₀ > 1 μM) (21).

Activity of vicriviroc against drug-resistant viruses. HIV-1 resistance to existing antiretroviral drugs is a growing problem in treatment-experienced patients, and new classes of active drugs are needed to effectively treat this population (25). Therefore, to demonstrate the activity of vicriviroc against drug-resistant viruses, we employed the PhenoSense assay (18). In this assay, pseudoviruses containing cloned RT and PR genes from treatment-experienced patients with reverse transcriptase inhibitor (RTI), protease inhibitor (PRI), or multi-drug resistance (MDR) mutations were generated using the envelope gene from the R5-tropic isolate JrCSF and tested for susceptibility to vicriviroc. Alternatively, viruses resistant to the fusion inhibitor enfuvirtide were generated with mutant JrCSF

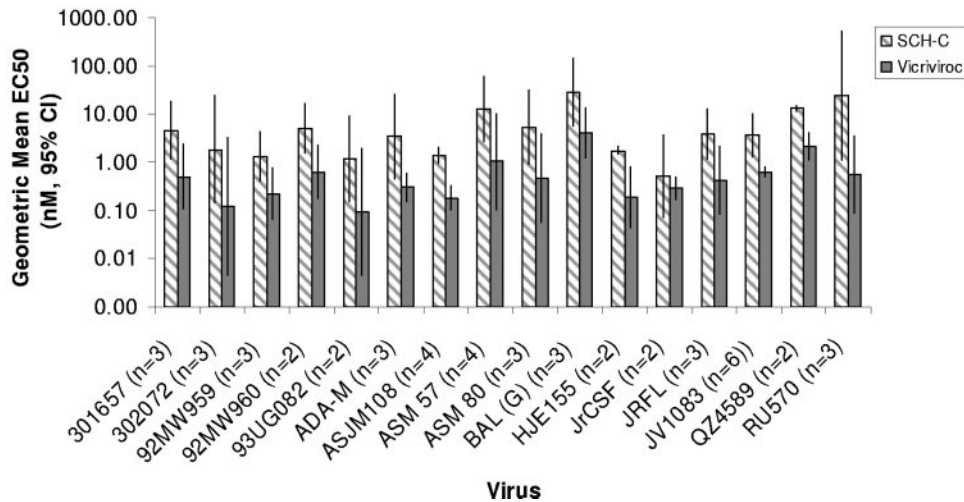


FIG. 4. Comparative antiviral activity of SCH-C and vicriviroc. The antiviral potencies of SCH-C (hatched bars) and vicriviroc (solid bars) were evaluated under identical conditions in the PBMC infection assay against a panel of HIV-1 isolates. The bars represent the geometric mean EC₅₀s determined for the indicated number experiments. Error bars represent the upper and lower boundaries of the 95% confidence interval (CI). Mean EC₅₀s for vicriviroc were 2- to 40-fold lower than SCH-C against all viruses tested.

TABLE 2. Antiviral activity of vicriviroc against HIV-1 pseudotyped viruses resistant to enfuvirtide, reverse transcriptase, and protease inhibitors

Virus tested	Phenotype ^a	Amino acid (aa) changes relative to WT			EC ₅₀ ^b (nM)	Fold change in IC ₅₀ ^c
		Reverse transcriptase (aa 1–305)	Protease (aa 1–99)	gp41 (aa 1–397)		
1	WT	WT	WT	WT	18.3	1.00
2	Enfuvirtide resistant	WT	WT	V38A	8.7	0.48
3	Enfuvirtide resistant	WT	WT	G36D, V38M	32.9	1.8
4	PR-RT MDR	V35V/I, T39E, M41L, E44D, D67N, K70R, L74I, K101P, Q102K, K103S, V118I, K122E, I135L, D177N, M184V, T200A, E203E/D/K/N, L210W, R211K, T215Y, D218E, K219E, L228H, R277K	L10I, T12P/S, I13V, L19P, K20M, L33I, E35D, M36I, N37D, M46M/I, G48V, I54T, I62I/V, L63P, I64V, T74S, V82A, N83N/S, T91T/S, I93I/M	WT	14.1	0.77
5	PR-RT MDR	P4S, V35L, M41L, E44D, D67N, K70R, L74I, V75S, K101E/Q, Q102K, L109I, V118I, K122E, I135V, C162S, V179F, Y181C, G190A, G196E, L210W, R211K, T215Y, D218E, K219E, L228H, Q242H, S251I, A272S, R277K, L283I, A288T	L10I, L33F, K43T, G48V, I50V, I54V, I62V, L63P, I64V, I72I/M, G73V, V77I, V82A, L90L/M	WT	12.3	0.67
6	RTI resistant	E6K, K20R, V35M, M41L, K43E, E44A, D67N, T69D, Q102K, V106I, T107S, L109I, V118I, K122E, I135T, R172K, K173N, Q174K, I178L, Y181C, M184V, Y188L, E203A, H208Y, L210W, R211K, T215Y, D218E, K219N, H221Y, L228H, R277K, T286A, V293I, E297K	L10L/I, V11V/I, L63P	WT	23.4	1.28
7	PI resistant	V35I, T39A, Q102K, V111I, K122E, C162S, F214L, S251I, R277K, V293I	L10F, L19L/I, K20M/R, L23L/I, E35E/D, M36I, R41R/K, M46L, I54V, I62I/V, L63P, A71V, V82A, I84I/V, L90M, I93L	WT	28.1	1.53

^a WT, wild type; PR, protease; RT, reverse transcriptase; MDR, multidrug resistant; RTI, RT inhibitor; PI, protease inhibitor.

^b Vicriviroc sensitivity against viral pools harboring the indicated mutations in the RT, PR, or gp41 genes, relative to the WT control virus, was determined using the PhenoSense assay (16). EC₅₀s were derived from a 9-point dose-response curve (concentration range, 0.01 to 667 nM; *n* = 2 wells/concentration) and are defined as the concentration of vicriviroc required to inhibit the mean luciferase signal by 50% relative to untreated control wells.

^c Fold change in EC₅₀ relative to the HIV pseudovirus generated with WT RT-PR and parental JrCSF envelope sequences.

envelope clones engineered to contain enfuvirtide resistance mutations (9). A summary of the RT, PR, and gp41 amino acid changes in the test viruses relative to the wild-type reference virus are shown in Table 2 along with the susceptibility data. Vicriviroc was active against the viruses with RTI, PRI, or MDR phenotypes, with EC₅₀s comparable to those of the wild-type control virus (Table 2). This result is expected, as vicriviroc targets an early step in the viral life cycle prior to reverse transcription and virion maturation, the targets of RTIs and PRIs, respectively. In addition, we assessed the ability of vicriviroc to inhibit enfuvirtide-resistant viruses in this assay. Vicriviroc was active against both the virus containing the gp41 V38A mutation as well as the virus with the double mutation (G36D and V28M) with EC₅₀s similar to (<2-fold) that obtained for the wild-type comparator virus.

Effect of vicriviroc in combination with other antiviral agents. Previously we reported that the earlier generated compound SCH-C showed synergistic activity when tested in combination with other antiretroviral agents (24). Similar analyses of vicriviroc were performed as part of the preclinical evaluation process. In this study, vicriviroc was evaluated in two-drug combinations, using representative drugs from all currently Food and Drug Administration-approved antiretroviral classes, nucleoside RTI (zidovudine and lamivudine), non-

nucleoside RTI (efavirenz), PRI (indinavir), and a fusion inhibitor (enfuvirtide). As illustrated in Table 3, combination index (CI) values ranged from 0.37 to 1.18 depending on the combination. All combinations tested showed synergistic interactions at EC₉₀ or above (concentrations of compound likely to be obtained clinically), with mean CI values ranging from 0.37 to 0.84. No toxicity was observed in the cultures at concentrations of up to 10 μM.

TABLE 3. Combination indices for vicriviroc and other antiretrovirals at various inhibitory concentrations against HIV R5-01

Drug ^a	EC ₅₀	EC ₇₅	EC ₉₀	EC ₉₅
Zidovudine	0.75 ± 0.20 ^b	0.58 ± 0.12	0.45 ± 0.07	0.37 ± 0.05
Lamivudine	0.73 ± 0.04	0.62 ± 0.03	0.56 ± 0.11	0.53 ± 0.16
Efavirenz	1.18 ± 0.03	0.98 ± 0.20	0.84 ± 0.32	0.76 ± 0.37
Indinavir	0.97 ± 0.02	0.88 ± 0.08	0.82 ± 0.11	0.80 ± 0.13
Enfuvirtide	0.94 ± 0.13	0.73 ± 0.06	0.60 ± 0.03	0.53 ± 0.06

^a Concentrations of vicriviroc ranged from 0.03 to 1.8 nM; zidovudine from 1 to 16 nM; lamivudine from 0.02 μM to 2.16 μM; efavirenz from 0.3 to 6.0 nM; indinavir from 5 to 72 nM; and enfuvirtide from 1 to 18 nM.

^b Combination index (CI) of <0.9 indicated synergy, between 0.9 and 1.1 indicated near additivity, and >1.1 indicated antagonism. Values represent the mean (±standard deviations) CI from two to four independent experiments.

TABLE 4. Comparative pharmacokinetic properties of SCH-C and vicriviroc

Parameter	SCH-C		Vicriviroc	
	Rat (10 mpk)	Monkey (2 mpk)	Rat (10 mpk)	Monkey (2 mpk)
Absorption (%)	57 ± 25 ^a	80 ± 34	100 ± 15	95 ± 14
Bioavailability (%)	63 ± 31	52 ± 50	100 ± 54	89 ± 13
C _{max} (μM)	2.5 (23%) ^b	0.76 (100%)	4.3 (8%)	1.3 (21%)
Half-life (h)	5.4 (16%)	6 (20%)	7.9 (28%)	3.4 (1%)

^a In vivo studies represent 3 animals; standard deviation (SD) values are reported for absorption and bioavailability and were calculated as follows: SD of bioavailability = bioavailability × [(SD of AUC_{oral}/AUC_{oral})² + (SD of AUC_{i.v.}/AUC_{i.v.})²]^{1/2}; SD of absorption = absorption × [(SD of AUC_{oral} radioactivity/AUC_{oral} radioactivity)² + (SD of AUC_{i.v.} radioactivity/AUC_{i.v.} radioactivity)²]^{1/2}.

^b Values in parentheses indicate % coefficient of variation.

Pharmacokinetic analysis. The pharmacokinetic properties of vicriviroc were determined in both rats and cynomolgus monkeys. The values for absorption, bioavailability, C_{max}, and plasma half-life are shown in Table 4. For comparison, we have included similar measurements previously reported for SCH-C (21). In both rats and monkeys, vicriviroc showed excellent absorption (95 to 100%) and oral bioavailability (89 to 100%), with C_{max} values of 1.3 μM in monkeys receiving a dose of 2 mg per kg body weight. This concentration is approximately 200-fold greater than the mean antiviral EC₉₀ concentration. The plasma half-life of vicriviroc was found to be somewhat shorter in monkeys than it was with SCH-C (3.4 h versus 6 h). Metabolism studies using human liver microsomes showed no significant inhibition of CYP450 liver enzymes by either SCH-C or vicriviroc. In addition, plasma protein binding of SCH-C and vicriviroc was found to be moderate, with approximately 16% of the compound remaining unbound in human plasma. Antiviral studies performed in the presence of increasing amounts of human serum showed no effect of serum concentration on the antiviral activity of vicriviroc at concentrations of up to 50% in the cultures (data not shown). Therefore, it is not anticipated that serum protein binding will have a significant impact on the antiviral efficacy of this compound in vivo.

Effect of vicriviroc on hERG current. In both preclinical safety studies and phase I human trials, it was noted that the prototypic compound SCH-C produced a mild prolongation of cardiac QTc intervals that were associated with peak plasma concentrations (C_{max}) in the highest dose groups. This effect is believed to be caused by inhibition of potassium flux through the hERG ion channel (8, 19). As part of the criteria for selection of the next-generation compound, candidates were screened for activity at this ion channel. As shown in Table 5

vicriviroc was nearly sixfold less active than SCH-C (IC₅₀ = 5.8 μM versus 1.1 μM) in attenuating hERG current in voltage-clamped L929 cells. This result demonstrates that vicriviroc has a lower affinity for this ion channel and suggests that vicriviroc is less likely to cause QTc changes in vivo than SCH-C.

DISCUSSION

Vicriviroc is a potent inhibitor of HIV-1 infection that acts by specifically blocking the viral coreceptor CCR5. In cell-based replication assays, vicriviroc exhibited broad-spectrum antiviral activity against a genotypically diverse panel of R5-tropic HIV-1 isolates with mean EC₅₀s ranging between 0.04 and 2.3 nM. In addition, vicriviroc was found to be significantly more potent than the earlier clinical compound, SCH-C. In head-to-head testing, vicriviroc was 2 to 40 times more potent than SCH-C against primary HIV isolates and was fully active against the Clade G isolate RU570, which has reduced susceptibility to SCH-C (21). These findings suggest that vicriviroc may be more effective in reducing viral titers in the clinic than SCH-C.

Since antiretroviral drugs are routinely dosed in combination as part of an optimized therapy regimen, we investigated the effect of drugs from other classes on the activity of vicriviroc. In vitro drug combination studies confirmed that vicriviroc acted synergistically with the RTIs zidovudine, lamivudine, and efavirenz and with the PRI indinavir. Additionally, vicriviroc was found to synergize with the fusion inhibitor enfuvirtide, demonstrating that targeting two steps in the entry process can have a cooperative effect. It has been speculated that, by stalling the fusion process, coreceptor inhibitors can potentiate the effects of fusion inhibitors by prolonging exposure of the conformational intermediate of gp41 targeted by enfuvirtide, thus enhancing its activity (5). Collectively, these findings suggest that vicriviroc may be used to enhance the activity of standard antiretroviral therapy regimens or as part of novel regimens to provide new treatment options for HIV-infected patients.

The issue of drug resistance continues to be a growing problem among HIV treatment-experienced individuals. Therefore, it is important that new therapies being developed for clinical use demonstrate activity against viruses with common drug resistance mutations. In this study, we evaluated vicriviroc against a panel of cloned viruses with defined RTI, PRI, or fusion inhibitor resistance patterns. As expected, vicriviroc was effective against all the viruses tested, including two multidrug-resistant strains. Furthermore, engineered viruses containing

TABLE 5. Comparative biophysical properties of SCH-C and vicriviroc

Assay	SCH-C	Vicriviroc
Protein binding (human plasma)	16% free (3%)	16% free (3.5%)
hERG (IC ₅₀)	1.1 μM ^a	5.8 μM
CYP 450 enzyme inhibition (IC ₅₀)	>30 μM	>30 μM

^a Concentration-response curve analysis for hERG activity by nonlinear regression of all data points: 0.11, 0.3, and 1.1 μM SCH-C resulted in an IC₅₀ of 1.1 μM (95% CI, 0.6 to 1.9 μM); 1, 3, and 10 μM vicriviroc revealed an IC₅₀ of 5.8 μM (95% CI, 4.7 to 7.2 μM). n = 4 to 5 replicates per drug concentration, and n = 5 to 7 per vehicle control group.

Downloaded from http://aac.asm.org/ on May 28, 2013 by guest

mutations in the gp41 gene associated with enfuvirtide resistance were completely sensitive to vicriviroc. These results further support a role for CCR5 antagonists in treatment-experienced patients; however, well-controlled and monitored studies will be necessary to assess the efficacy and durability of this new class of compounds in patients.

To characterize the interaction of vicriviroc with CCR5 more completely, we performed a series of receptor binding and functional activity studies. In three different functional assays, chemotaxis, calcium flux, and GTP γ S binding, vicriviroc potently inhibited the activation of CCR5 by its natural ligands, RANTES, MIP-1 α , and MIP-1 β , with activity in the low-nanomolar range. Vicriviroc alone did not activate the receptor in any of the functional assays, thus demonstrating it is a pure receptor antagonist. Interestingly, with the exception of the GTP γ S exchange assay, there was little discernible difference between vicriviroc and SCH-C activity in these analyses despite the fact that vicriviroc was more active than SCH-C against primary HIV-1 infection. The chemotaxis and calcium flux assays each employed relatively brief drug incubation times that are unlikely to accurately reflect the *in vivo* situation. To evaluate any potential advantage of prolonged incubation sufficient to permit a steady-state drug receptor equilibrium, membranes expressing CCR5 were preincubated with SCH-C or vicriviroc for 24 h prior to the initiation of GTP γ S exchange. Under this paradigm, vicriviroc was a more potent antagonist of CCR5 activation than was SCH-C. In order to model the prolonged drug exposure *in vivo*, a time course analysis of compound affinity was carried out. These studies clearly showed that at shorter incubation times, vicriviroc appeared to have lower affinity and bind more slowly to CCR5 than SCH-C. However, once equilibrium binding was reached (about 24 h), vicriviroc showed an approximately threefold greater affinity for CCR5. This suggests that while vicriviroc may initially bind more slowly to the receptor, once bound it binds more tightly and remains bound to the receptor longer. The higher affinity and slower off-rate likely accounts for vicriviroc's enhanced antiviral activity compared to that of SCH-C that was observed in the cell-based infection assays.

Since convenience in dosing is an important consideration for all new antiretroviral agents in development, it was important that our selected clinical candidate compound possess a favorable pharmacokinetic profile compared to that of SCH-C. *In vivo* animal dosing studies indicated that vicriviroc had excellent oral bioavailability and absorption properties in both rats and monkeys and that plasma levels attained were many fold in excess of the IC₉₀s required for antiviral activity. In addition to its favorable pharmacokinetics profile, vicriviroc was not found to inhibit key liver drug metabolizing enzymes, including CYP 3A4 or 2C9. Therefore, vicriviroc is not expected to influence the concentrations of other agents when used as part of an antiretroviral cocktail, a finding that was recently confirmed in several drug interaction studies (A. Sansone, Abstr. 6th Int. Workshop Clin. Pharmacol. HIV Ther., presentation 6.4, 2005). Taken together, the favorable pharmacokinetic and drug metabolism profiles of vicriviroc support further development of this compound.

Finally, we evaluated vicriviroc in a patch-clamp model of L929 cells to assess its ability to block hERG channel current, a potential cause of QTc prolongation. Our findings showed

that vicriviroc was nearly sixfold less active in this assay than SCH-C. Furthermore, electrocardiograph studies in preclinical animal models have shown no effect of vicriviroc on QTc intervals at plasma concentrations as high as 3.6 μ M in monkeys and 6 μ M in dogs. (R. Johnson and A. Keung, personal communication). The QTc prolongation observed with SCH-C is likely to be compound specific and not a mechanism-based effect.

In summary, the findings reported here show that vicriviroc is a potent antagonist of the CCR5 receptor, possessing broad-spectrum antiviral activity. This, in conjunction with favorable pharmacokinetic properties, supports the further development of vicriviroc as a novel antiviral agent for the treatment of HIV-1 infection.

ACKNOWLEDGMENTS

We thank T. C. Chou, A. Keung, M. Laughlin, R. Johnson, and A. Sansone for their contributions to the manuscript. In addition, we appreciate the efforts of R. Mayer-Ezell, L. Dunkle, W. R. Bishop, and Ferdous Gheyas for their editorial comments.

REFERENCES

- Cheng, Y., and W. H. Prusoff. 1973. Relationship between the inhibition constant (K_i) and the concentration of inhibitor which causes 50 per cent inhibition (I₅₀) of an enzyme reaction. *Biochem. Pharmacol.* **22**:3099–3108.
- Chou, T. C. 1991. The median-effect principle and the combination index for quantitation of synergism and antagonism, p. 61–102. *In* T. C. Chou and D. C. Rideout (ed.), *Synergism and antagonism in chemotherapy*. Academic Press, San Diego, Calif.
- Cox, M. A., C.-H. Jenh, W. Gonsiorek, J. Fine, S. K. Narula, P. J. Zavodny, and R. W. Hipkin. 2001. Human interferon-inducible 10-kDa protein and human interferon-inducible T cell α chemoattractant are allotropic ligands for human CXCR3: differential binding to receptor states. *Mol. Pharmacol.* **59**:707–715.
- Doms, R. W. 2001. Chemokine receptors and HIV entry. *AIDS* **15**(Suppl. 1): S34–S35.
- Doms, R. W., and J. P. Moore. 2000. HIV-1 membrane fusion: targets of opportunity. *J. Cell Biol.* **151**:F9–F14.
- Eron, J. J., R. M. Gulick, J. A. Bartlett, T. Merigan, R. Arduino, J. M. Kilby, B. Yangco, A. Diers, C. Drobnes, R. DeMasi, M. Greenberg, T. Melby, C. Raskino, P. Rusnak, Y. Zhang, R. Spence, and G. D. Miralles. 2004. Short-term safety and antiretroviral activity of T-1249, a second-generation fusion inhibitor of HIV. *J. Infect. Dis.* **189**:1075–1083.
- Este, J. A. 2003. Virus entry as a target for anti-HIV intervention. *Curr. Med. Chem.* **10**:1617–1632.
- Finlayson, K., H. J. Witchel, J. McCulloch, and J. Sharkey. 2004. Acquired QT interval prolongation and HERG: implications for drug discovery and development. *Eur. J. Pharmacol.* **500**:129–142.
- Greenberg, M. L., and N. Cammack. 2004. Resistance to enfuvirtide, the first HIV fusion inhibitor. *J. Antimicrob. Chemother.* **54**:333–340.
- Hendrix, C. W., A. C. Collier, M. M. Lederman, D. Schols, R. B. Pollard, S. Brown, J. B. Jackson, R. W. Coombs, M. J. Glesby, C. W. Flexner, G. J. Bridger, K. Badel, R. T. MacFarland, G. W. Henson, and G. f. t. A. H. S. G. Calandra. 2004. Safety, pharmacokinetics and antiviral activity of AMD3100, a selective CXCR4 receptor inhibitor, in HIV-1 infection. *J. Acquir. Immun. Defic. Syndr.* **37**:1253–1262.
- Jacobson, J. M., R. J. Israel, I. Lowy, N. A. Ostrow, L. S. Vassilatos, M. Barish, D. N. Tran, B. M. Sullivan, T. J. Ketas, T. J. O'Neill, K. A. Nagashima, W. Huang, C. J. Petropoulos, J. P. Moore, P. J. Maddon, and W. C. Olson. 2004. Treatment of advanced human immunodeficiency virus type 1 disease with the viral entry inhibitor PRO 542. *Antimicrob. Agents Chemother.* **48**:423–429.
- Kilby, J. M., S. Hopkins, T. M. Venetta, B. DiMassimo, G. A. Cloud, J. Y. Lee, L. Alldredge, E. Hunter, D. Lambert, D. Bolognesi, T. Matthews, M. R. Johnson, M. A. Nowak, G. M. Shaw, and M. S. Saag. 1998. Potent suppression of HIV-1 replication in humans by T-20, a peptide inhibitor of gp41-mediated virus entry. *Nat. Med.* **4**:1302–1307.
- Lalezari, J. P., M. Thompson, P. Kumar, P. Piliero, R. Davey, K. Patterson, A. Shachoy-Clark, K. Adkison, J. Demarest, Y. Lou, M. Berrey, and S. Piscitelli. 2005. Antiviral activity and safety of 873140, a novel CCR5 antagonist, during short-term monotherapy in HIV-infected adults. *AIDS* **19**: 1443–1448.
- Lazzarin, A., B. Clotet, D. Cooper, J. Reynes, K. Arasteh, M. Nelson, C. Katlama, H.-J. Stellbrink, J.-F. Delfraissy, J. Lange, L. Huson, R. DeMasi, C. Wat, J. Delehanty, C. Drobnes, M. Salgo, and the TORO 2 Study Group.

2003. Efficacy of enfuvirtide in patients infected with drug-resistant HIV-1 in Europe and Australia. *N. Engl. J. Med.* **348**:2186–2195.
15. Lin, P.-F., W. Blair, T. Wang, T. Spicer, Q. Guo, N. Zhou, Y.-F. Gong, H.-G. H. Wang, R. Rose, G. Yamanaka, B. Robinson, C.-B. Li, R. Fridell, C. Deminie, G. Demers, Z. Yang, L. Zadjura, N. Meanwell, and R. Colonno. 2003. A small molecule HIV-1 inhibitor that targets the HIV-1 envelope and inhibits CD4 receptor binding. *Proc. Natl. Acad. Sci. USA*. **100**:11013–11018.
 16. Maeda, K., H. Nakata, H. Ogata, Y. Koh, T. Miyakawa, and H. Mitsuya. 2004. The current status of, and challenges in, the development of CCR5 inhibitors as therapeutics for HIV infection. *Curr. Opin. Pharmacol.* **4**:447–452.
 17. Palani, A., S. Shapiro, J. W. Clader, W. J. Greenlee, K. Cox, J. Strizki, M. Endres, and B. M. Baroudy. 2001. Discovery of 4-[(Z)-(4-bromophenyl)-(ethoxymino)methyl]-1'-[(2,4-dimethyl-3-pyridinyl)carbonyl]-4'-methyl-1,4'-bipiperidine N-oxide (SCH 351125): an orally bioavailable human CCR5 antagonist for the treatment of HIV infection. *J. Med. Chem.* **44**:3339–3342.
 18. Petropoulos, C. J., N. T. Parkin, K. L. Limoli, Y. S. Lie, T. Wrin, W. Huang, H. Tian, D. Smith, G. A. Winslow, D. J. Capon, and J. M. Whitcomb. 2000. A novel phenotypic drug susceptibility assay for human immunodeficiency virus type 1. *Antimicrob. Agents Chemother.* **44**:920–928.
 19. Redfern, W. S., L. Carlsson, A. S. Davis, W. G. Lynch, I. MacKenzie, S. Palenthorpe, P. K. S. Siegl, I. Strang, A. T. Sullivan, R. Wallis, A. J. Camm, and T. G. Hammond. 2003. Relationships between preclinical cardiac electrophysiology, clinical QT interval prolongation and torsade de pointes for a broad range of drugs: evidence for a provisional safety margin in drug development. *Cardiovasc. Res.* **58**:32–45.
 20. Root, M. J., M. S. Kay, and P. S. Kim. 2001. Protein design of an HIV-1 entry inhibitor. *Science* **291**:884–888.
 21. Strizki, J. M., S. Xu, N. E. Wagner, L. Wojcik, J. Liu, Y. Hou, M. Endres, A. Palani, S. Shapiro, J. W. Clader, W. J. Greenlee, J. R. Tagat, S. McCombie, K. Cox, A. B. Fawzi, C. C. Chou, C. Pugliese-Sivo, L. Davies, M. E. Moreno, D. D. Ho, A. Trkola, C. A. Stoddart, J. P. Moore, G. R. Reyes, and B. M. Baroudy. 2001. SCH-C (SCH 351125), an orally bioavailable, small molecule antagonist of the chemokine receptor CCR5, is a potent inhibitor of HIV-1 infection in vitro and in vivo. *Proc. Natl. Acad. Sci. USA* **98**:12718–12723.
 22. Tagat, J. R., S. W. McCombie, D. Nazareno, M. A. Labroli, Y. Xiao, R. W. Steensma, J. M. Strizki, B. M. Baroudy, K. Cox, J. Lachowicz, G. Varty, and R. Watkins. 2004. Piperazine-based CCR5 antagonists as HIV-1 inhibitors. IV. Discovery of 1-[(4,6-dimethyl-5-pyrimidinyl)carbonyl]-4-[4-[2-methoxy-1(R)-4-(trifluoromethyl)phenyl]ethyl-3(S)-methyl-1-piperazinyl]-4-methyl-piperidine (Sch-417690/Sch-D), a potent, highly selective, and orally bioavailable CCR5 antagonist. *J. Med. Chem.* **47**:2405–2408.
 23. Tagat, J. R., S. W. McCombie, R. W. Steensma, S. Lin, D. V. Nazareno, B. Baroudy, N. Vantuno, S. Xu, and J. Liu. 2001. Piperazine-based CCR5 antagonists as HIV-1 inhibitors. I: 2(S)-methyl piperazine as a key pharmacophore element. *Bioorg. Med. Chem. Lett.* **11**:2143–2146.
 24. Tremblay, C. L., F. Giguel, C. Kollmann, Y. Guan, T. C. Chou, B. M. Baroudy, and M. S. Hirsch. 2002. Anti-human immunodeficiency virus interactions of SCH-C (SCH 351125), a CCR5 antagonist, with other antiretroviral agents in vitro. *Antimicrob. Agents Chemother.* **46**:1336–1339.
 25. United Kingdom Collaborative Group on HIV Drug Resistance. 2005. Estimating HIV-1 drug resistance in antiretroviral-treated individuals in the United Kingdom. *J. Infect. Dis.* **192**:967–973.
 26. Wild, C., D. Shugars, T. Greenwell, C. McDanal, and T. Matthews. 1994. Peptides corresponding to a predictive α -helical domain of human immunodeficiency virus type 1 gp41 are potent inhibitors of virus infection. *Proc. Natl. Acad. Sci. USA* **91**:9770–9774.